




## Nuclear spectroscopy with heavy ion nucleon knockout and (p,2p) reactions

Jianguo Li <sup>1,\*</sup> Carlos A. Bertulani <sup>2,3,†</sup> and Furong Xu <sup>1,‡</sup>

<sup>1</sup>*School of Physics, and State Key Laboratory of Nuclear Physics and Technology, Peking University, Beijing 100871, China*

<sup>2</sup>*Department of Physics and Astronomy, Texas A&M University-Commerce, Texas 75429-3011, USA*

<sup>3</sup>*Institut für Kernphysik, Technische Universität Darmstadt, D-64289 Darmstadt, Germany*



(Received 9 October 2021; revised 9 January 2022; accepted 8 February 2022; published 22 February 2022)

Knockout reactions with heavy ion targets in inverse kinematics, as well as “quasifree” (p,2p) and (p,pn) reactions are useful tools for nuclear spectroscopy. We report calculations on *ab initio* many-body wave functions based on the no-core shell model to study the nucleon removal reactions in light nuclei, including beryllium, carbon, and oxygen isotopic chains, and explore the importance of using an *ab initio* method. Our study helps to clarify how the extraction of spectroscopic factors from the experiments depend on the details of the many-body wave functions being probed. We show that recent advances with the *ab initio* method can provide more insights on the spectroscopy information extracted from experiments.

DOI: [10.1103/PhysRevC.105.024613](https://doi.org/10.1103/PhysRevC.105.024613)

### I. INTRODUCTION

Heavy ion nucleon reactions in which an impinging nucleus has one of its nucleons removed by a hard collision with a target nucleus have become a standard spectroscopic tool. The so-called nucleon knockout is particularly useful to study reactions with radioactive nuclear beams. Another much celebrated spectroscopic tool is (p,2p) or (p,pn) reactions, using hydrogen targets for studies involving nuclei far from the stability [1]. Various subjects of interest for nuclear physics have been assessed with knockout and quasifree (p,2p) and (p,pn) reactions such as magicity, shell evolution, and the structure of loosely bound nuclei, short-range correlations [2,3]. Since the first experimental campaigns using radioactive beams in knockout reactions [4–6], the community has used absolute value of cross sections, as well as the momentum distributions of the fragment core to identify the quantum numbers of the removed nucleon, as well as the details of the nuclear wave functions [7–21].

In direct reactions, the amplitude of the overlap function of the bound-state wave functions of the initial and final nuclei is the telltale of the total nuclear wave functions and interaction potentials. The overlap functions are defined as

$$\begin{aligned} I_{lj}(r) &= \langle \Psi_A^{J_A} | [ | \Psi_{A-1}^{J_{A-1}} \rangle \otimes | l, j \rangle^{J_A} ] \rangle, \\ &= \sum_i \langle \Psi_A^{J_A} | a_{n,lj}^\dagger | | \Psi_{A-1}^{J_{A-1}} \rangle \langle n_i l j | u_i \rangle, \end{aligned} \quad (1)$$

where  $|\Psi_A^{J_A}\rangle$  and  $|\Psi_{A-1}^{J_{A-1}}\rangle$  are wave functions of the nuclei  $A$  and  $A-1$ , respectively. The  $a_{n,lj}^\dagger$  is a creation operator associated with the single-particle basis state  $|u_i\rangle$ . Within Eq. (1), the overlap function involves summation over all the

single-particle states with the same  $lj$  quantum number. The final integrals have small dependence of the single-particle basis assumed, which are in contrast to the standard shell-model calculations within a limited model space where the model dependence enters through the specific choice of a single-particle state  $|nlj\rangle$ , with Eq. (1) reducing to a single matrix elements  $\langle \Psi_A^{J_A} | a_{n,lj}^\dagger(i) | | \Psi_{A-1}^{J_{A-1}} \rangle$  [22]. Note that  $I_{lj}(r)$  is not an eigenfunction of a Hermitian Hamiltonian and cannot be directly associated with a probability. Thus, it is not normalized to unity and the spectroscopic factor for the nuclear configuration, defined as

$$C^2 S_{lj} = \int dr r^2 |I_{lj}(r)|^2, \quad (2)$$

can be larger than unity. The  $C^2 S$  is a model-dependent quantity that can be calculated in the shell model, being sensitive to the interactions and to the truncations of the model space. They usually differ from unity because they depend on the contribution of numerous antisymmetrized and different nonorthogonal channels coupled to the two-body  $n(A-1)$  channel.

At a large distance  $r$ , the overlap function is proportional to the Whittaker function, depending only on the charge of the particles, the binding energy, and a normalization constant, i.e.,

$$I_{lj}(r) \longrightarrow C_{lj} \frac{1}{r} W_{-\eta, l+1/2}(2\kappa r), \quad (3)$$

with  $\mu$  being the nucleon +  $(A-1)$  nucleus reduced mass,  $\eta = \mu Z_n Z_{A-1} e^2 / \hbar \kappa$  the Sommerfeld parameter,  $\kappa = \sqrt{2\mu E_B} / \hbar$  the wave number,  $E_B$  the nucleon separation energy,  $Z_{A-1}$  and  $Z_n$  the residual nucleus and nucleon charges, and  $l$  the nucleon angular momentum. Thus, at large distances,  $|I_{lj}|^2$  should be proportional to the square of the normalization coefficients (ANC):  $C_{lj}^2$ . It is often stated that, due to their peripheral character, heavy ion knockout reactions are directly proportional to  $C^2$ , although this view is not confirmed by

\*jianguo\_li@pku.edu.cn

†carlos.bertulani@tamuc.edu

‡frxu@pku.edu.cn

detailed calculations [23]. In fact, it was already noted that the single-neutron knockout reactions from  $^{10}\text{C}$  and  $^{10}\text{Be}$  beams incident on light nuclear targets have demonstrated a sensitivity to differences in shell-model, no-core shell model (NCSM), and variational Monte Carlo (VMC) wave functions and therefore may help the development of *ab initio* structure models [24]. In this work we concentrate on how theory can provide an accurate account of the spectroscopic quantities, defined in Eqs. (1) and (2). This is timely, as a “quenching” of the spectroscopic factors in heavy ion knockout reactions has become a hot topic in the recent literature [1,9,25], although (p,2p) reactions seem to contradict these findings [17–19,21]. Here we explore the impact on the experimental analysis in the case one uses *ab initio* wave functions to calculate both heavy ion knockout and (p,2p) reactions.

New experiments using (p,pN) reactions, with  $N = p, n$ , in inverse kinematics have been reported [17–19,21], being accompanied by new developments in reaction theories using different models than those adopted for heavy ion knockout reactions. In particular, (p,pN) reactions are more sensitive to the inner part of the nuclear wave function [23], specially for light nuclear projectiles [17,18,26]. This has been clearly discussed in Refs. [23,26]. One thus expects that (p,pN) reactions involve an increased sensitivity to the many-body aspects of the single-particle content of the nuclear wave functions. The sole knowledge of spectroscopic factors is not enough for a good description of (p,pN) reactions and in some cases even for heavy ion knockout reactions. We use the reaction theory reported in Refs. [27,28] for the heavy ion knockout, and in Ref. [26] for the (p,2p) case. Other variants of these reactions models are found in Refs. [29–42]. The input of these calculations are the nucleon-nucleon cross sections, using the parametrization provided in Ref. [43], and nuclear densities calculated with the *ab initio* procedure. It is worthwhile mentioning that the cross section obtained here depend very little ( $\lesssim 5\%$ ) on the differences between densities obtained with the *ab initio* and other methods, such as neutron/proton ratio scaled densities obtained from electron-scattering experiments. Therefore, the calculations are a major probe of the nuclear wave functions and their respective overlap integrals, as in Eq. (1).

## II. OVERLAP FUNCTIONS WITH AN *AB INITIO* METHOD

### A. *Ab initio* wave functions

The *ab initio* NCSM [44] has been employed. Contrary to the standard shell-model in which the calculations are performed within limited model space using an inner frozen core, the NCSM calculations are done without a core and the model space is as large as possible to obtain the converged results within the ability of supercomputer [44–46]. The correct treatment of internucleon correlations is one of the strongest features of the NCSM calculations within a large model space. In contrast, only configuration mixings within a small model space are considered in the standard shell-model calculations. The nucleon orbital occupations are spread over a large space in the NCSM, but in the standard shell-model only single-particle orbitals within the restricted model space

are occupied. In the NCSM, the center-of-mass correction is made using the Lawson method [44]. In the present work, we perform the NCSM using the Daejeon16 interaction [47] which could provide good descriptions of light nuclei, to compute the energies, overlap functions and  $C^2S$  values for the states. The results for these quantities are shown in Table. I.

It is well known that *ab initio* wave functions obtained from expansions in harmonic-oscillator wave functions have a hard time reproducing the large distance behavior of the nuclear states and a large number of basis functions need to be used for the purpose. This does not diminish the merit of using such wave functions neither for quasifree (p,pN) reactions nor for knockout reactions with heavy ions. The bulk (but not all) of the cross sections in heavy ion knockout reactions are due to the tail of the overlap integrals. Therefore, this tail has to be reproduced well. This can be easily fixed [49,50] by using a procedure that replaces *ab initio* wave functions at their tails by those with appropriate asymptotic behavior such as solutions of a Woods-Saxon model. A fit extending to the internal part of the *ab initio* overlap functions yield and adequate renormalization yield correct knockout cross sections. In the case of (p,pN) reactions, an accurate description of the overlap integral tail is not of relevance for the total cross sections, as the bulk of the cross sections are due to the inner part of the overlap integral.

Following Ref. [51], we define a reduction factor  $R$  as the ratio of the experimental cross section to theoretical prediction; usually  $R < 1$  due to correlations between the nucleons. Elaborated shell-model (SM) calculations have not been able to explain the reductions obtained for  $R$  or the quenching of spectroscopic factors (SF). An overall reduction of SFs compared with the SM has been observed, e.g., in Refs. [9,25].

### B. Results and discussions

In Tables II–XI we present our results for the calculations comparing them to the experimental data.

In Table II we show the comparison of our calculations and experimental data for proton (neutron) knockout from  $^7\text{Li}$  projectiles incident on  $^9\text{Be}$  targets. Our calculated spectroscopic factors and cross sections for the specified states are given in the sixth and seventh columns. For the  $^9\text{Be}(^7\text{Li}, ^6\text{He})$  reaction at 80 MeV/nucleon, our results are remarkably close to those reported in Ref. [48] using wave functions calculated with the variational Monte Carlo (VMC) method [56]. We get 28.13 mb, while the value quoted in Ref. [48] using VMC wave functions is 26.7 mb. Our spectroscopic factor for the  $0^+$  state in the residual nucleus is 0.496 and 0.439 for the VMC method. The experimental cross section is only 13.3(5) mb, one of the smallest nucleon knockout reaction cross sections probably related to  $^7\text{Li}$  having a prominent  $\alpha$ -triton cluster structure in contrast with  $^6\text{He}$  having a halo structure with an  $\alpha$ -core and two loosely bound neutrons. The transition between the  $^7\text{Li}$  and  $^6\text{He}$  ground states through the knockout of a proton must be a fine-tuning reaction mechanism, not well described by the reaction models neglecting couplings to other channels such as the dissociation of  $^6\text{He}$  as pointed out in Ref. [48].

TABLE I. Theoretical and experimental total energies ( $E$ , in MeV) and calculated  $C^2S$  values for the nuclear states studied in this work.  $N_{\max}$  indicates the harmonic-oscillator basis space used in the NCSM calculations. The nucleus (left) added by one proton or neutron becomes the nucleus on the right. The asterisk \* indicates that this coupling cannot exist. An oscillator basis with  $\hbar\omega = 15$  MeV is used for the Daejeon16 interaction.

Nucleus	State	$E_{\text{expt}}$	$E_{\text{theor}}$	$N_{\max}$	Nucleus	State	$E_{\text{expt}}$	$E_{\text{theor}}$	$N_{\max}$	$C^2S(p_{3/2})$	$C^2S(p_{1/2})$
${}^6\text{He}$	$0^+$	-29.27	-28.98	12	${}^7\text{Li}$	$3/2^-$	-39.25	-39.08	10	0.50	*
${}^6\text{Li}$	$1^+$	-31.99	-31.57	12						0.47	0.18
	$0^+$	-28.43	-28.00	12						0.25	*
${}^7\text{Be}$	$3/2^-$	-37.60	-40.14	10	${}^8\text{B}$	$2^+$	-37.74	-39.99	10	0.76	0.07
	$1/2^-$	-37.17	-39.89	10						0.23	*
${}^8\text{B}$	$2^+$	-37.74	-39.99	10	${}^9\text{C}$	$3/2^-$	-39.04	-39.71	8	0.88	0.04
${}^8\text{Li}$	$2^+$	-41.28	-42.85	10	${}^9\text{Li}$	$3/2^-$	-45.34	-45.79	8	0.90	0.04
	$1^+$	-40.30	-41.89	10						0.30	0.00
${}^9\text{Li}$	$3/2^-$	-45.34	-45.79	8	${}^{10}\text{Be}$	$0^+$	-64.98	-67.40	8	1.38	*
	$1/2^-$	-42.69	-44.62	8						*	0.42
${}^9\text{C}$	$3/2^-$	-39.04	-39.71	8	${}^{10}\text{C}$	$0^+$	-60.32	-62.89	8	1.34	*
${}^{11}\text{B}$	$3/2^-$	-76.21	-74.50	6	${}^{12}\text{C}$	$0^+$	-92.16	-91.30	6	2.69	*
${}^{11}\text{C}$	$3/2^-$	-73.44	-71.80	6						2.50	*
${}^{13}\text{N}$	$1/2^-$	-94.11	-95.26	6	${}^{14}\text{O}$	$0^+$	-98.73	-99.05	6	*	1.53
${}^{13}\text{O}$	$3/2^-$	-75.55	-73.20	6						3.23	*
${}^{15}\text{N}$	$1/2^-$	-115.49	-115.43	6	${}^{16}\text{O}$	$0^+$	-127.62	-129.79	6	*	1.58
	$3/2^-$	-105.17	-105.96	6						3.07	*
${}^{15}\text{O}$	$1/2^-$	-111.96	-113.22	6						*	1.70
	$3/2^-$	-105.78	-103.30	6						3.21	*

For the  ${}^9\text{Be}({}^7\text{Li}, {}^6\text{Li})$  reaction at 120 MeV/nucleon our calculations yield 61.21 mb while with VMC wave functions one obtains 52.6 mb, and 53.8 with shell-model wave functions. The spectroscopic factors for the  $1^+$  state are 0.649 compared with 0.715 with the VMC. For the  $0^+$  state these numbers are 0.250 and 0.219, respectively. These values are much closer than those obtained with the shell-model calculations, in agreement with the analysis made in Ref. [48]. The small differences found should not be ascribed to the reaction calculations but to the details of the *ab initio* wave functions, which do not perfectly agree with each other. But it is worth noticing that the calculations using shell-model, VMC and NCSM wave functions overestimate the cross sections compared with the experimental value of 30.7 mb. There is no clear explanation for the disagreement between theory and experiment.

In Table III we show the comparison of our calculations and experimental data for proton knockout from  ${}^8\text{B}$  projectiles incident on  ${}^{12}\text{C}$  targets at different beam energies. Our calculated spectroscopic factors and cross sections for the specified states are given in the sixth and seventh columns. The proton is assumed to be removed from either the  $j = 3/2$  or the  $j = 1/2$  orbital of the  ${}^8\text{B}$  ground state. In our model, the  $2^+$  ground state in  ${}^8\text{B}$  is an admixture of contributions from the  $3/2$  and  $1/2$  orbitals. The residual nucleus  ${}^7\text{Be}$  is left either in its  $3/2^-$  ground state or in its  $1/2^-$  excited state at 429 keV. It is worthwhile comparing our results with the theoretical calculations for the same reactions (except the one for 76 MeV/nucleon) as reported in Ref. [51]. We notice the same bombarding energy dependence of the cross sections, decreasing to a minimum at 285 MeV/nucleon before increasing again. This is an expected feature reminiscent of

TABLE II. Proton (neutron) knockout with  ${}^7\text{Li}$  projectiles. The computed reduction factor  $R$  is the ratio between the experimental and theoretical inclusive one-nucleon-removal cross sections.  $C^2S(\text{th})$  indicates that the spectroscopic factors are computed using the NCSM.  $C^2S(\text{VMC})$  denotes that the results are calculated with the VMC.

Reaction	$E_{\text{beam}}$ MeV/nucleon	$J^\pi$	$j$	$S_p[S_n]$ MeV	$C^2S(\text{th})$	$C^2S(\text{VMC})$	$\sigma_{\text{theor}}$ mb	$\sigma_{\text{expt}}$ mb	$R$
${}^9\text{Be}({}^7\text{Li}, {}^6\text{He})$ [48]	80	$0^+$	$3/2$	9.98	0.496	0.439	28.13	13.4 (7)	0.476 (24)
${}^9\text{Be}({}^7\text{Li}, {}^6\text{Li})$ [48]	120	$1^+$	$1/2$	7.25	0.176	0.24	15.21		
			$3/2$		0.473	0.47	28.91		
		$0^+$	$3/2$	10.8	0.250	0.219	17.09		
		Inclusive					61.21	30.7 (18)	0.501(29)

TABLE III. Proton (neutron) knockout with  $^8\text{Be}$  projectiles.

Reaction	$E_{\text{beam}}$ MeV/nucleon	$J^\pi$	$j$	$S_n$ MeV	$C^2S(\text{th})$	$\sigma_{\text{theor}}$ mb	$\sigma_{\text{expt}}$ mb	$R$
$^{12}\text{C}(^8\text{B}, ^7\text{Be})$ [52]	76	$3/2^-$	3/2	0.137	0.761	53.98		
			1/2		0.073	28.53		
			3/2	0.559	0.227	25.26		
$^{12}\text{C}(^8\text{B}, ^7\text{Be})$ [53]	142	$3/2^-$	Inclusive			107.78	130(11)	1.206(102)
			3/2	0.137	0.761	54.57		
			1/2		0.073	19.87		
$^{12}\text{C}(^8\text{B}, ^7\text{Be})$ [53]	285	$3/2^-$	3/2	0.559	0.227	21.75		
			Inclusive			96.19	109(1)	1.133(10)
			3/2	0.137	0.761	47.64		
$^{12}\text{C}(^8\text{B}, ^7\text{Be})$ [54]	936	$3/2^-$	3/2	0.559	0.225	16.96		
			Inclusive			77.23	89(2)	1.154(13)
			3/2	0.137	0.761	47.06		
$^{12}\text{C}(^8\text{B}, ^7\text{Be})$ [54]	936	$3/2^-$	3/2	0.137	0.761	15.26		
			1/2		0.073	17.64		
			3/2	0.559	0.225	79.96	94(9)	1.176(112)
$^{12}\text{C}(^8\text{B}, ^7\text{Be})$ [55]	1440	$3/2^-$	3/2	0.137	0.761	48.81		
			1/2		0.073	18.07		
			3/2	0.559	0.225	19.19		
$^{12}\text{C}(^8\text{B}, ^7\text{Be})$ [55]	1440	$3/2^-$	Inclusive			86.07	96(3)	1.115 (34)
			3/2	0.137	0.761	48.81		
			1/2		0.073	18.07		

the energy dependence of the nucleon-nucleon cross section. But our cross sections are consistently smaller, by about 20% than the theoretical results obtained with shell-model wave functions reported in Ref. [51].

One of the possible explanations for this disagreement is the very small proton separation energy. It is often stated that the NCSM wave functions do not properly describe the long tails of loosely bound states in light nuclei because they are based on an expansion in harmonic oscillator basis which naturally display a quick falloff at large distances. However, the internucleon correlations are well treated within the NCSM. This was indeed shown in Refs. [49,50] where the problem was fixed by matching the NCSM wave functions with the expected tails well described by Whittaker functions. This trick

allowed a good reproduction of the momentum distributions and cross sections for knockout reactions with  $^8\text{B}$  projectiles. Another noteworthy observation is that our spectroscopic factors are very close to those shell-model results in Ref. [51], except for that of the  $j = 3/2$  and the  $3/2^-$  ground state of  $^7\text{Be}$ . Our numerical value is 0.761 while Ref. [51] indicated a spectroscopic factor of 0.97. The model used in Ref. [51] is directly related to the spectroscopic factor [see Eq. (1) in Ref. [51]]. In the present work, the Glauber model [27,28] is used, in which the overlap integrals acts as the input information. This could be a possible reason for the difference.

In Table IV we show the comparison of our calculations with experimental data for proton knockout from  $^9\text{C}$  projectiles incident on  $^{12}\text{C}$  targets. Our calculated spectroscopic

TABLE IV. Knockout reactions with  $A = 9$  projectiles.

Reaction	$E_{\text{beam}}$ MeV/nucleon	$J^\pi$	$j$	$S_p[S_n]$ MeV	$C^2S(\text{th})$	$\sigma_{\text{theor}}$ mb	$\sigma_{\text{expt}}$ mb	$R$
$^{12}\text{C}(^9\text{C}, ^8\text{B})$ [52]	78	$2^+$	3/2	1.3	0.876	42.24		
			1/2		0.042	13.96		
			Inclusive			56.2	54 (4)	0.961(71)
$^9\text{Be}(^9\text{C}, ^8\text{B})$ [48]	100	$2^+$	3/2	1.3	0.876	46.21		
			1/2		0.042	10.68		
			Inclusive			56.9	56 (3)	0.984(53)
$^9\text{Be}(^9\text{Li}, ^8\text{Li})$ [48]	80	$2^+$	3/2	4.06	0.895	36.38		
			1/2		0.042	8.758		
			3/2	5.05	0.026	5.423		
$^{12}\text{C}(^9\text{Li}, ^8\text{Li})$ [48]	100	$2^+$	3/2	4.06	0.895	50.56	55.6(29)	1.100(57)
			1/2		0.040	10.94		
			3/2	5.05	0.026	6.90		
$^{12}\text{C}(^9\text{Li}, ^8\text{Li})$ [48]	100	$2^+$	Inclusive			65.66	62.9(41)	0.958(62)
			3/2	4.06	0.895	47.82		
			1/2		0.040	10.94		

TABLE V. Knockout reactions with  $A = 10$  projectiles.

Reaction	$E_{\text{beam}}$ MeV/nucleon	$J^\pi$	$j$	$S_p[S_n]$ MeV	$C^2S(\text{th})$	$C^2S(\text{VMC})$	$C^2S(\text{SM})$	$\sigma_{\text{theor}}$ mb	$\sigma_{\text{expt}}$ mb	$R$
${}^9\text{Be}({}^{10}\text{Be}, {}^9\text{Li})$ [48]	80	$3/2^-$	$3/2$	19.64	1.375	1.043	1.929	41.37		
		$1/2^-$	$1/2$	22.33	0.424	0.434	0.282	18.30		
${}^9\text{Be}({}^{10}\text{Be}, {}^9\text{Be})$ [48]	120	$3/2^-$	$3/2$	6.812	2.148	1.963	2.622	59.67	26.0(13)	0.435(22)
	80							66.54	69.5(32)	1.045(45)
${}^9\text{Be}({}^{10}\text{C}, {}^9\text{C})$ [48]	120	$3/2^-$	$3/2$	21.28	1.340	1.043	1.933	48.98	23.4(11)	0.478(22)
${}^{12}\text{C}({}^{10}\text{C}, {}^9\text{C})$ [48]	120	$3/2^-$	$3/2$	21.28	1.340	1.043	1.933	55.63	27.4(13)	0.492(23)

TABLE VI. Knockout reactions with  $A = 12$  projectiles.

Reaction	$E_{\text{beam}}$ MeV/nucleon	$J^\pi$	$j$	$S_p[S_n]$ MeV	$C^2S(\text{th})$	$\sigma_{\text{theor}}$ mb	$\sigma_{\text{expt}}$ mb	$R$
${}^{12}\text{C}({}^{12}\text{C}, {}^{11}\text{B})$ [57]	250	$3/2^-$	$3/2$	15.95	2.690	77.31	65.6(26)	0.849(34)
${}^{12}\text{C}({}^{12}\text{C}, {}^{11}\text{B})$ [20]	400					67.44	60.9(27)	0.903(40)
${}^{12}\text{C}({}^{12}\text{C}, {}^{11}\text{B})$ [58]	1050					61.89	48.6(24)	0.785(38)
	2100					62.58	53.8(27)	0.860(43)
${}^{12}\text{C}({}^{12}\text{C}, {}^{11}\text{C})$ [57]	250	$3/2^-$	$3/2$	18.72	2.497	78.19	56.0(41)	0.716(52)
${}^{12}\text{C}({}^{12}\text{C}, {}^{11}\text{C})$ [58]	1050					61.54	44.7(28)	0.726(45)
	2100					62.03	46.5(23)	0.750(37)

TABLE VII. Knockout reactions with  $A = 14$  projectiles.

Reaction	$E_{\text{beam}}$ MeV/nucleon	$J^\pi$	$j$	$S_p[S_n]$ MeV	$C^2S(\text{th})$	$C^2S(\text{SM})$	$\sigma_{\text{theor}}$ mb	$\sigma_{\text{expt}}$ mb	$R$
${}^{12}\text{C}({}^{14}\text{O}, {}^{13}\text{N})$ [61]	305	$1/2^-$	$1/2$	4.63	1.531	1.55	39.66	35(5)	0.883(126)
${}^9\text{Be}({}^{14}\text{O}, {}^{13}\text{N})$ [62]	53						36.29	58(4)	1.607(110)
${}^9\text{Be}({}^{14}\text{O}, {}^{13}\text{O})$ [62]	53	$3/2^-$	$3/2$	23.18	3.234	3.15	31.34	14(4)	0.465(127)

TABLE VIII. Knockout reactions with  $A = 16$  projectiles.

Reaction	$E_{\text{beam}}$ MeV/nucleon	$J^\pi$	$j$	$S_p(S_n)$ MeV	$C^2S(\text{th})$	$\sigma_{\text{theor}}$ mb	$\sigma_{\text{expt}}$ mb	$R$
${}^{12}\text{C}({}^{16}\text{O}, {}^{15}\text{N})$ [57]	2100	$1/2^-$	$1/2$	12.13	1.581	28.83		
		$3/2^-$	$3/2$	22.04	3.066	49.84		
${}^{12}\text{C}({}^{16}\text{O}, {}^{15}\text{O})$ [58]	2100	Inclusive				78.67	54.2(29)	0.689(37)
		$1/2^-$	$1/2$	12.13	1.702	30.41		
		$3/2^-$	$3/2$	22.04	3.209	47.58		
		Inclusive				77.99	42.9(23)	0.550(29)

TABLE IX. Quasifree (p,2p) and (p,pn) reactions with  ${}^{12}\text{C}$ .

Reaction	$E_{\text{beam}}$ MeV/nucleon	$J^\pi$	$j$	$S_p(S_n)$ MeV	$C^2S(\text{th})$	$\sigma_{\text{theor}}$ mb	$\sigma_{\text{expt}}$ mb	$R$
${}^{12}\text{C}(\text{p},2\text{p}){}^{11}\text{B}$ [18]	400	$3/2^-$	$3/2$	15.96	2.497	16.23	15.8(18)	
		$1/2^-$	$1/2$	18.08	0.475	2.492	1.9(2)	
		Inclusive				18.72	17.7(18)	0.945(96)
${}^{12}\text{C}(\text{p}, \text{pn}){}^{11}\text{C}$ [21]	400	$3/2^-$	$3/2$	18.72	2.686	24.16		
		$1/2^-$	$1/2$	21.40	0.512	4.457		
		Inclusive				28.62	30.0(32)(27)	1.048(206)



TABLE X. (p,2p) reactions with oxygen isotopes. Experimental cross sections are from Ref. [17], listed along with statistical (round brackets) and systematic uncertainties (square brackets).

Reaction	$E_{\text{beam}}$ MeV/nucleon	$J^\pi$	$j$	$S_p$ MeV	$C^2S(\text{th})$	$\sigma_{\text{theor}}$ mb	$\sigma_{\text{expt}}$ mb	$R$
$^{14}\text{O}(p, 2p)^{13}\text{N}$ [17]	351	$1/2^-$	1/2	4.626	1.532	16.58	10.23(0.80)[0.65]	0.617(87)
$^{16}\text{O}(p, 2p)^{15}\text{N}$ [17]	451	$1/2^-$	1/2	12.13	1.581	12.24		
		$3/2^-$	3/2	18.76	3.209	16.69		
		Inclusive				28.93	26.84(0.90)[1.70]	0.928(89)

factors and cross sections for the specified states are given in the sixth and seventh columns. The proton is assumed to be removed from either the  $j = 3/2$  or the  $j = 1/2$  orbital of the  $^9\text{C}$   $3/2^-$  ground state with a proton separation energy of 1.3 MeV. Both reactions  $^{12}\text{C}(^9\text{C}, ^8\text{B})X$  and  $^9\text{Be}(^9\text{C}, ^8\text{B})X$  have similar experimental values and our calculations using NCSM wave functions are in excellent agreement with the experiments. According to Ref. [48] the proton knockout  $^9\text{Be}(^9\text{C}, ^8\text{B})X$  at 100 MeV/nucleon calculated with VMC

TABLE XI. The computed reduction factor  $R$ ,  $\Delta S = S_p - S_n$  for neutron removal or  $\Delta S = S_p - S_n$  for proton removal.

Reaction	$\Delta S$ MeV	$E_{\text{beam}}$ MeV/nucleon	$R$
$^9\text{B}(^7\text{Li}, ^6\text{He})$	2.723	80	0.476(24)
$^9\text{B}(^7\text{Li}, ^6\text{Li})$	-2.723	120	0.501(29)
$^{12}\text{C}(^8\text{B}, ^7\text{Be})$	-12.690	76	1.206(102)
		142	1.133(10)
		285	1.154(13)
		936	1.176(112)
		1440	1.115(34)
$^{12}\text{C}(^9\text{C}, ^8\text{B})$	-12.925	78	0.961(71)
$^9\text{Be}(^9\text{C}, ^8\text{B})$	-12.690	100	0.984(53)
$^9\text{Be}(^9\text{Li}, ^8\text{Li})$	-9.882	80	1.100(57)
$^{12}\text{C}(^9\text{Li}, ^8\text{Li})$	-9.882	100	0.958(62)
$^9\text{Be}(^{10}\text{Be}, ^9\text{Li})$	12.824	80	0.435(22)
$^9\text{Be}(^{10}\text{Be}, ^9\text{Be})$	-12.824	80	1.045(45)
		120	0.810(48)
$^9\text{Be}(^{10}\text{C}, ^9\text{C})$	17.277	120	0.478(22)
$^{12}\text{C}(^{10}\text{C}, ^9\text{C})$	17.277	120	0.492(23)
$^{12}\text{C}(^{12}\text{C}, ^{11}\text{B})$	-2.764	250	0.849(34)
		400	0.903(40)
		1050	0.785(38)
		2100	0.860(43)
$^{12}\text{C}(^{12}\text{C}, ^{11}\text{C})$	2.764	250	0.716(52)
		1050	0.726(45)
		2100	0.750(37)
$^{12}\text{C}(^{14}\text{O}, ^{13}\text{N})$	-18.552	305	0.883(126)
$^9\text{Be}(^{14}\text{O}, ^{13}\text{N})$	-18.552	53	1.607(110)
$^9\text{Be}(^{14}\text{O}, ^{13}\text{O})$	18.552	53	0.465(127)
$^{12}\text{C}(^{16}\text{O}, ^{15}\text{N})$	-3.537	2100	0.689(37)
$^{12}\text{C}(^{16}\text{O}, ^{15}\text{O})$	3.537	2100	0.550(29)
$^{12}\text{C}(p, 2p)^{11}\text{B}$	-2.764	400	0.945(96)
$^{12}\text{C}(p, pn)^{11}\text{C}$	2.764	400	1.048(206)
$^{14}\text{O}(p, 2p)^{13}\text{N}$	-18.552	351	0.617(87)
$^{16}\text{O}(p, 2p)^{15}\text{N}$	-3.537	451	0.928(89)

wave functions [56] is 64.4(15) mb, about 20% larger than the experimental values. The cross sections calculated with the shell model for  $^{12}\text{C}(^9\text{C}, ^8\text{B})X$  at 78 MeV/nucleon is 65.7 mb, as reported in Ref. [52]. Our results are much closer to the experimental data, yielding a much smaller reduction factor  $R = \sigma_{\text{expt}}/\sigma_{\text{theor}}$ .

The reaction ( $^9\text{Li}, ^8\text{Li}$ ) is mirror symmetric with respect to ( $^9\text{C}, ^8\text{B}$ ) and the measured and calculated cross sections are nearly equal, despite an additional excited state in  $^8\text{Li}$ . Because of the mirror symmetry, the spectroscopic factors for the  $2^+$  state are almost identical. But one notices that the neutron removal from the  $1^+$  state adds an extra 6 mb to the ( $^9\text{Li}, ^8\text{Li}$ ) reaction, which is absent in the ( $^9\text{C}, ^8\text{B}$ ) reaction. This is substantial smaller than the 20 mb value for the removal from the  $1^+$  state reported in Ref. [48]. Therefore, our calculations are in accordance with the mirror symmetry and the expected cross sections are concentrated in the same  $2^+$  state, as expected from the symmetry.

In Table V we show the comparison of our calculations with experimental data for knockout reactions with  $A = 10$  projectiles on  $^9\text{Be}$  and  $^{12}\text{C}$  targets. The ( $^{10}\text{Be}, ^9\text{Li}$ ) proton knockout reaction is the mirror reaction to ( $^{10}\text{C}, ^9\text{C}$ ). The ( $^{10}\text{Be}, ^9\text{Li}$ ) reaction with a proton removal from the  $0^+$  state can populate the  $3/2^-$  ground state of  $^9\text{Li}$ , as well as its excited state at 2.69 MeV. Our spectroscopic factors are similar to the VMC calculations reported in Ref. [48], although for the  $3/2^-$  states they are about 20% smaller, whereas the VMC and shell-model spectroscopic factors differ by up to a factor of two. However, our calculated cross section is about the same percentage larger than the VMC. The VMC theoretical cross section adds up to 50.3 mb, whereas our result is 59.67 mb. Both calculations overpredict the experimental value of 26.0(13) mb, as observed in Ref. [48].

The ( $^{10}\text{Be}, ^9\text{Be}$ ) reaction with a neutron removal from the  $0^+$  state can populate the  $3/2^-$  ground state of  $^9\text{Be}$ , with a neutron separation energy of 6.81 MeV. Our spectroscopic factor of 2.148 lies between the shell model and the VMC respective values of 2.622 and 1.932 reported in Ref. [48]. The cross sections obtained with our wave function are 66.54 and 88.08 mb, at 80 and 120 MeV/nucleon, respectively. These results also lie between the shell-model and VMC values and are in reasonable agreement with the experimental data.

The ( $^{10}\text{C}, ^9\text{C}$ ) reaction with a neutron removal from the  $0^+$  state can populate the  $3/2^-$  ground state of  $^9\text{C}$ , with a neutron separation energy of 21.28 MeV. Our spectroscopic factor of 1.340 once more lies between the shell-model and the VMC respective values of 1.933 and 1.043 reported in Ref. [48]. The cross sections obtained with our wave function is

48.98 mb for Be targets and 120 MeV/nucleon  $^{10}\text{C}$  projectiles and 55.63 mb and for C targets. These results are closer to those obtained with VMC wave functions but are again larger by about a factor of two than the experimental data.

In Table VI we compare our calculations to the inclusive reaction cross sections for nucleon removal from  $^{12}\text{C}$  projectiles incident on carbon targets at 250, 400, 1050, and 2100 MeV/nucleon, as reported in Refs. [20,57,58]. All particle removals are assumed to take place from the  $p_{3/2}$  orbitals. But it is worthwhile mentioning that all these data are inclusive, with no identification of the orbitals from which the nucleons are removed. Our calculated spectroscopic factors and cross sections for the specified states are given in the sixth and seventh columns. It is noticeable that the calculated cross sections are about 10%–20% larger for the proton removal case of  $^{12}\text{C}(^{12}\text{C}, ^{11}\text{B})$  and substantially larger for neutron removal cases of  $^{12}\text{C}(^{12}\text{C}, ^{11}\text{C})$ . Nonetheless, our theoretical calculations yield very similar results as those reported in previous references, as in Ref. [59] where a quantum molecular dynamics (QMD) model was used for comparison with the experimental data. The physics included in our theoretical model is not easy to translate into those included in QMD. The QMD model assumes wave packets for nucleons incorporating momentum-dependent forces, surface tension, and a Pauli “force” into the Hamiltonian as effective potential terms. The model is popular in investigate multifragmentation reactions in nucleus-nucleus collisions. A common problem with the model is the inaccurate treatment of peripheral collisions attributed to spurious excitation and disintegration of nuclei. Such effects could not be distinguished from the true events arising from peripheral collisions [60]. These drawbacks were apparently fixed in Ref. [59] and it is remarkable that despite the very different modeling, their results are in the same ballpark as ours.

In Table VII we compare our calculations to the inclusive cross sections for nucleon removal from  $^{14}\text{O}$  projectiles incident on beryllium and carbon targets at 53 and 305 MeV/nucleon, as reported in Refs. [61,62]. We assume that the neutrons are removed from the  $p_{3/2}$  orbital, whereas the proton is removed from the  $p_{1/2}$  orbital. Our calculated spectroscopic factors and cross sections for the specified states are given in the sixth and seventh columns. Calculations based on the intranuclear cascade method [63] predict for the  $^{12}\text{C}(^{14}\text{O}, ^{13}\text{N})$  reaction at 305 MeV/nucleon a cross section of 39 MeV, assuming a scaled geometry, as explained in Ref. [61]. This is amazingly close to our calculated value of 39.66 mb, despite the differences in the reaction models used. However, the experimental cross section, as reported in Ref. [62] for the  $^9\text{Be}(^{14}\text{O}, ^{13}\text{N})$  reaction at 53 MeV/nucleon is 58(4) mb, contrasting sharply with the one published Ref. [61]. The cross section for  $^{12}\text{C}(^{14}\text{O}, ^{13}\text{N})$  at 53 MeV/nucleon as reported in Ref. [62] is very different from our calculated value and also from their own eikonal calculations. Our calculated value of 36.29 mb for this reaction is consistent with the expectation that is the energy dependence of the nucleon-nucleon cross section, which decreases rapidly as the beam energy increases from 50 to 300 MeV/nucleon. Since the eikonal model used here yields similar cross sections as the intranuclear cascade model at

305 MeV/nucleon, it is hard to pinpoint where the source of discrepancy might be. For more discussions on this, see Ref. [61]. The situation is inverted for the  $^9\text{Be}(^{14}\text{O}, ^{13}\text{O})$  reaction at 53 MeV/nucleon, with our calculated cross section value of 31.34 mb whereas the experimental cross section is 14(4) mb. Both our calculations of the spectroscopic factor and cross section are close to the results in Ref. [7,62].

In Table VIII we compare our calculations to the inclusive cross sections for nucleon removal from  $^{16}\text{O}$  projectiles incident on beryllium and carbon targets at 53 and 305 MeV/nucleon, as reported in Refs. [57,58]. The nucleons are removed from the  $p_{3/2}$  and  $p_{1/2}$  orbitals. Our calculated spectroscopic factors and cross sections for the specified states are given in the sixth and seventh columns. The calculated values are in rather good agreement with the experimental data for the reaction  $^{12}\text{C}(^{16}\text{O}, ^{15}\text{N})$  at 2100 MeV/nucleon, whereas an appreciably larger enhancement factor of the theoretical cross section is observed for the neutron removal reaction  $^{12}\text{C}(^{16}\text{O}, ^{15}\text{O})$  at the same energy.

We now turn on to quasifree reactions of the (p,2p) and (p,pn) type in inverse kinematics. In Table IX we compare our calculations to the quasifree cross sections for  $^{12}\text{C}(p, 2p)^{11}\text{Be}$  and  $^{12}\text{C}(p, pn)^{11}\text{C}$  reaction reported in Refs. [18,21]. The reaction part of the calculations follow the theory developed in Ref. [26]. The nucleons are assumed to be removed from the  $1p_{3/2}$  and  $1p_{1/2}$  orbitals, for both cases. For the  $^{12}\text{C}(p, 2p)^{11}\text{Be}$  reaction the sum of our calculated spectroscopic factors is equal to 2.97 whereas the value quoted in Ref. [21] is  $\sum C^2S = 4.28$  based on the shell-model calculated with the Warburton-Brown interaction [64] in the *spstdpf* model space restricted to  $(0 + 1)\hbar\omega$ . The agreement with our results are outstanding. But the summed set of spectroscopic factors are very different. We notice that in Refs. [18,21] the calculations reported were done using a Woods-Saxon wave function and spectroscopic factors from shell models. In our case, we have used wave functions calculated with the no-core shell model for consistency. As recently discussed in Ref. [23], the quasifree cross sections are strongly dependent of the form of the wave functions, and not only the spectroscopic factors. Therefore, we deem the agreement between the two sets of calculations (shell model and *ab initio*) as being coincidental for these two reactions.

To reinforce the arguments raised above, in Table X we list cross sections for (p,2p) reactions with oxygen isotopes. Experimental cross sections are from Ref. [17], presented along with statistical (round brackets) and systematic uncertainties (square brackets). All protons are assumed to be removed from the  $1p_{1/2}$  orbital, except for the  $^{16}\text{O}$  case, where they are assumed to be removed from a mixture of the  $1p_{1/2}$  orbital (ground state) and from  $1p_{3/2}$  orbital corresponding to two excited states at 6.63 and 9.93 MeV, with the inclusive cross section listed for the sum of their contributions. For  $^{16}\text{O}(p, 2p)^{15}\text{N}$ , the states with separation energies 18.76 and 22.06 MeV are considered as part of a single mixed state. As in the previous data of Table IX, the calculations reported in Ref. [17] do not use *ab initio* wave functions but those generated with Woods-Saxon potentials scaled with spectroscopic factors for the *ab initio* self-consistent Green’s function (SCGF) method. Our calculated cross sections use not only

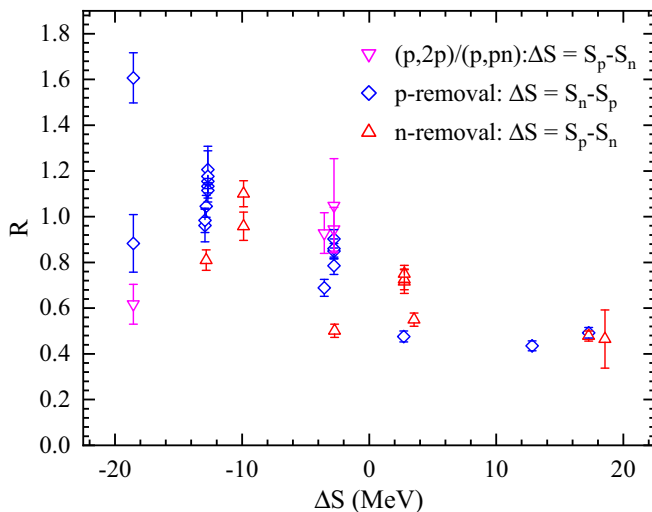


FIG. 1. Compilation of the computed reduction factors between the experimental and theoretical inclusive one-nucleon-removal cross sections. Blue, red, and pink symbols are for the proton removal, neutron removal, and (p,2p) [or (p,pn)], respectively.

the spectroscopic factors from the *ab initio* NCSM but also the wave functions generated in the model. Our results are about 20% smaller than the theoretical results using SCGF spectroscopic factors [65,66] as reported in Ref. [17]. This again reinforces the idea of the importance of using proper *ab initio* wave functions for a consistent analysis of the experimental data.

### III. CONCLUSIONS

(p,pN) probes are much more sensitive to the details of the internal part of the overlap functions than knockout by heavy targets. But the latter type of reactions is also influenced by the internal details of the overlap functions. A close inspection of Tables II–X reveals that substantial agreements exist in the experimental reduction factors for heavy-ion-induced reactions obtained with wave functions generated with many-body overlap functions. The calculated reduction factors for reactions investigated in the present work are summarized in Fig. 1 and Table XI. There is a small tendency of the reduc-

tion factor for (p,pN) reactions to increase with  $\Delta S$ , whereas this trend is reversed for heavy ion knockout reactions, in accordance with the findings of Refs. [9,25]. Furthermore, we reinforce the notion that nucleon removal in heavy ion knockout reactions cannot be only ascribed to the asymptotic behavior of the wave functions. A simple rescaling of the tails of the wave function with an ANC or by multiplication with spectroscopic factors can lead to a misidentification of important nuclear structure effects imbedded in the overlap functions. Therefore, the whole picture of quenching of spectroscopic factors might be misleading if Woods-Saxon wave functions, or wave-function tails, are used in the analysis. This assertion indicates that future experimental analyses of nucleon removal in (p,pN) and heavy ion knockout reactions require a closer collaboration of experiment and *ab initio* theory practitioners than typically reported in the literature.

In summary, we have shown that a proper experimental analysis requires the input of a properly calculated overlap function from first principles. While this poses a more difficult task for the study of single-particle configurations with (p,pN) reactions, it also opens opportunities for a better understanding of the nucleon-nucleon correlation effects in the overlap functions.

### ACKNOWLEDGMENTS

The NCSM code was provided by N. Michel, which is publicly available (see Ref. [67]). We also acknowledge J. P. Vary and P. Maris for providing us the Daejeon16 interaction. This work has been supported by the National Key R&D Program of China under Grant No. 2018YFA0404401; the National Natural Science Foundation of China under Grants No. 11835001, No. 11921006, No. 12035001, and No. 11975282; the State Key Laboratory of Nuclear Physics and Technology, Peking University under Grant No. NPT2020KFY13; the Strategic Priority Research Program of Chinese Academy of Sciences under Grant No. XDB34000000; and the CUSTIPEN (China-U.S. Theory Institute for Physics with Exotic Nuclei) funded by the U.S. Department of Energy, Office of Science under Grant No. de-sc0009971; the U.S. DOE grant DE-FG02-08ER41533. We acknowledge the High-Performance Computing Platform of Peking University for providing computational resources.

- 
- [1] T. Aumann *et al.*, *Prog. Part. Nucl. Phys.* **118**, 103847 (2021).  
 [2] M. Duer *et al.* (CLAS Collaboration), *Phys. Rev. Lett.* **122**, 172502 (2019).  
 [3] M. Patsyuk *et al.*, *Nat. Phys.* **17**, 693 (2021).  
 [4] K. Riisager *et al.*, *Nucl. Phys. A* **540**, 365 (1992).  
 [5] N. A. Orr, N. Anantaraman, S. M. Austin, C. A. Bertulani, K. Hanold, J. H. Kelley, D. J. Morrissey, B. M. Sherrill, G. A. Souliotis, M. Thoennessen, J. S. Winfield, and J. A. Winger, *Phys. Rev. Lett.* **69**, 2050 (1992).  
 [6] D. Bazin, R. J. Charity, R. T. de Souza, M. A. Famiano, A. Gade, V. Henzl, D. Henzllova, S. Hudan, H. C. Lee, S. Lukyanov, W. G. Lynch, S. McDaniel, M. Mocko, A. Obertelli, A. M. Rogers, L. G. Sobotka, J. R. Terry, J. A. Tostevin, M. B. Tsang, and M. S. Wallace, *Phys. Rev. Lett.* **102**, 232501 (2009).  
 [7] F. Flavigny, A. Gillibert, L. Nalpas, A. Obertelli, N. Keeley, C. Barbieri, D. Beaumel, S. Boissinot, G. Burgunder, A. Cipollone, A. Corsi, J. Gibelin, S. Giron, J. Guillot, F. Hammache, V. Lapoux, A. Matta, E. C. Pollacco, R. Raabe, M. Rejmund, N. de Sereville, A. Shrivastava, A. Signoracci, and Y. Utsuno, *Phys. Rev. Lett.* **110**, 122503 (2013).  
 [8] A. Bonaccorso, R. J. Charity, R. Kumar, and G. Salvioni, *AIP Conf. Proc.* **1645**, 30 (2015).  
 [9] J. A. Tostevin and A. Gade, *Phys. Rev. C* **103**, 054610 (2021).  
 [10] M. B. Tsang, J. Lee, S. C. Su, J. Y. Dai, M. Horoi, H. Liu, W. G. Lynch, and S. Warren, *Phys. Rev. Lett.* **102**, 062501 (2009).  
 [11] T. Otsuka, A. Gade, O. Sorlin, T. Suzuki, and Y. Utsuno, *Rev. Mod. Phys.* **92**, 015002 (2020).



- [12] J. Lee, M. B. Tsang, D. Bazin, D. Coupland, V. Henzl, D. Henzlova, M. Kilburn, W. G. Lynch, A. M. Rogers, A. Sanetullaev, Z. Y. Sun, M. Youngs, R. J. Charity, L. G. Sobotka, M. Famiano, S. Hudan, D. Shapira, P. O'Malley, W. A. Peters, K. Y. Chae, and K. Schmitt, *Phys. Rev. C* **83**, 014606 (2011).
- [13] S. Kawase *et al.*, *Prog. Theor. Exp. Phys.* **2018**, 021D01 (2018).
- [14] Y. X. Zhao, Y. Z. Sun, S. T. Wang, Z. Y. Sun, X. H. Zhang, D. Yan, D. Y. Pang, P. Ma, Y. H. Yu, K. Yue, S. W. Tang, S. M. Wang, F. Fang, Y. Sun, Z. H. Cheng, X. M. Liu, H. R. Yang, C. G. Lu, and L. M. Duan, *Phys. Rev. C* **100**, 044609 (2019).
- [15] A. Mutschler, O. Sorlin, A. Lemasson, D. Bazin, C. Borcea, R. Borcea, A. Gade, H. Iwasaki, E. Khan, A. Lepailleur, F. Recchia, T. Roger, F. Rotaru, M. Stanoiu, S. R. Stroberg, J. A. Tostevin, M. Vandebrouck, D. Weisshaar, and K. Wimmer, *Phys. Rev. C* **93**, 034333 (2016).
- [16] J. Lee, M. B. Tsang, D. Bazin, D. Coupland, V. Henzl, D. Henzlova, M. Kilburn, W. G. Lynch, A. M. Rogers, A. Sanetullaev, A. Signoracci, Z. Y. Sun, M. Youngs, K. Y. Chae, R. J. Charity, H. K. Cheung, M. Famiano, S. Hudan, P. O'Malley, W. A. Peters, K. Schmitt, D. Shapira, and L. G. Sobotka, *Phys. Rev. Lett.* **104**, 112701 (2010).
- [17] L. Atar *et al.* (R3B Collaboration), *Phys. Rev. Lett.* **120**, 052501 (2018).
- [18] V. Panin *et al.*, *Phys. Lett. B* **753**, 204 (2016).
- [19] D. D. Fernández *et al.* (R3B Collaboration), *Phys. Rev. C* **97**, 024311 (2018).
- [20] V. Panin *et al.*, *Phys. Lett. B* **797**, 134802 (2019).
- [21] M. Holl *et al.*, *Phys. Lett. B* **795**, 682 (2019).
- [22] E. Caurier, G. Martínez-Pinedo, F. Nowack, A. Poves, and A. P. Zuker, *Rev. Mod. Phys.* **77**, 427 (2005).
- [23] C. A. Bertulani, A. Idini, and C. Barbieri, *Phys. Rev. C* **104**, L061602 (2021).
- [24] G. F. Grinyer, D. Bazin, A. Gade, J. A. Tostevin, P. Adrich, M. D. Bowen, B. A. Brown, C. M. Campbell, J. M. Cook, T. Glasmacher, S. McDaniel, P. Navrátil, A. Obertelli, S. Quaglioni, K. Siwek, J. R. Terry, D. Weisshaar, and R. B. Wiringa, *Phys. Rev. Lett.* **106**, 162502 (2011).
- [25] J. A. Tostevin and A. Gade, *Phys. Rev. C* **90**, 057602 (2014).
- [26] T. Aumann, C. A. Bertulani, and J. Ryckebusch, *Phys. Rev. C* **88**, 064610 (2013).
- [27] P. G. Hansen and J. A. Tostevin, *Annu. Rev. Nucl. Part. Sci.* **53**, 219 (2003).
- [28] C. Bertulani and A. Gade, *Comput. Phys. Commun.* **175**, 372 (2006).
- [29] C. A. Bertulani and K. W. McVoy, *Phys. Rev. C* **46**, 2638 (1992).
- [30] G. Krein, T. A. J. Maris, B. B. Rodrigues, and E. A. Veit, *Phys. Rev. C* **51**, 2646 (1995).
- [31] E. Cravo, R. Crespo, and A. Deltuva, *Phys. Rev. C* **93**, 054612 (2016).
- [32] H. Esbensen, *Phys. Rev. C* **53**, 2007 (1996).
- [33] K. Hencken, G. Bertsch, and H. Esbensen, *Phys. Rev. C* **54**, 3043 (1996).
- [34] M. Gomez-Ramos and A. Moro, *Phys. Lett. B* **785**, 511 (2018).
- [35] C. A. Bertulani and P. G. Hansen, *Phys. Rev. C* **70**, 034609 (2004).
- [36] K. Ogata, K. Yoshida, and K. Minomo, *Phys. Rev. C* **92**, 034616 (2015).
- [37] J. Lei and A. Bonaccorso, *Phys. Lett. B* **813**, 136032 (2021).
- [38] A. M. Moro, *Phys. Rev. C* **92**, 044605 (2015).
- [39] K. Minomo, M. Kohno, K. Yoshida, and K. Ogata, *Phys. Rev. C* **96**, 024609 (2017).
- [40] R. Crespo, E. Cravo, and A. Deltuva, *Phys. Rev. C* **99**, 054622 (2019).
- [41] C. Hebborn and P. Capel, *J. Phys.: Conf. Ser.* **1643**, 012088 (2020).
- [42] C. Hebborn and P. Capel, *Phys. Rev. C* **104**, 024616 (2021).
- [43] C. A. Bertulani and C. De Conti, *Phys. Rev. C* **81**, 064603 (2010).
- [44] B. R. Barrett, P. Navrátil, and J. P. Vary, *Prog. Part. Nucl. Phys.* **69**, 131 (2013).
- [45] J. G. Li, N. Michel, B. S. Hu, W. Zuo, and F. R. Xu, *Phys. Rev. C* **100**, 054313 (2019).
- [46] J. G. Li, N. Michel, W. Zuo, and F. R. Xu, *Phys. Rev. C* **104**, 024319 (2021).
- [47] A. Shirokov, I. Shin, Y. Kim, M. Sosonkina, P. Maris, and J. Vary, *Phys. Lett. B* **761**, 87 (2016).
- [48] G. F. Grinyer, D. Bazin, A. Gade, J. A. Tostevin, P. Adrich, M. D. Bowen, B. A. Brown, C. M. Campbell, J. M. Cook, T. Glasmacher, S. McDaniel, A. Obertelli, K. Siwek, J. R. Terry, D. Weisshaar, and R. B. Wiringa, *Phys. Rev. C* **86**, 024315 (2012).
- [49] P. Navrátil, C. Bertulani, and E. Caurier, *Phys. Lett. B* **634**, 191 (2006).
- [50] P. Navrátil, C. A. Bertulani, and E. Caurier, *Phys. Rev. C* **73**, 065801 (2006).
- [51] B. A. Brown, P. G. Hansen, B. M. Sherrill, and J. A. Tostevin, *Phys. Rev. C* **65**, 061601(R) (2002).
- [52] J. Enders, T. Baumann, B. A. Brown, N. H. Frank, P. G. Hansen, P. R. Heckman, B. M. Sherrill, A. Stolz, M. Thoennessen, J. A. Tostevin, E. J. Tryggestad, S. Typel, and M. S. Wallace, *Phys. Rev. C* **67**, 064301 (2003).
- [53] B. Blank *et al.*, *Nucl. Phys. A* **624**, 242 (1997).
- [54] D. Cortina-Gil *et al.*, *Phys. Lett. B* **529**, 36 (2002).
- [55] D. Cortina-Gil *et al.*, *Eur. Phys. J. A* **10**, 49 (2001).
- [56] S. C. Pieper and R. B. Wiringa, *Annu. Rev. Nucl. Part. Sci.* **51**, 53 (2001).
- [57] J. M. Kidd, P. J. Lindstrom, H. J. Crawford, and G. Woods, *Phys. Rev. C* **37**, 2613 (1988).
- [58] D. L. Olson, B. L. Berman, D. E. Greiner, H. H. Heckman, P. J. Lindstrom, and H. J. Crawford, *Phys. Rev. C* **28**, 1602 (1983).
- [59] T. Ogawa, T. Sato, S. Hashimoto, D. Satoh, S. Tsuda, and K. Niita, *Phys. Rev. C* **92**, 024614 (2015).
- [60] W. R. Webber, J. C. Kish, and D. A. Schrier, *Phys. Rev. C* **41**, 547 (1990).
- [61] Z. Y. Sun, D. Yan, S. T. Wang, S. W. Tang, X. H. Zhang, Y. H. Yu, K. Yue, L. X. Liu, Y. Zhou, F. Fang, J. D. Chen, J. L. Chen, P. Ma, and C. G. Lu, *Phys. Rev. C* **90**, 037601 (2014).
- [62] F. Flavigny, A. Obertelli, A. Bonaccorso, G. F. Grinyer, C. Louchart, L. Nalpas, and A. Signoracci, *Phys. Rev. Lett.* **108**, 252501 (2012).
- [63] C. Louchart, A. Obertelli, A. Boudard, and F. Flavigny, *Phys. Rev. C* **83**, 011601(R) (2011).
- [64] E. K. Warburton and B. A. Brown, *Phys. Rev. C* **46**, 923 (1992).
- [65] C. Barbieri and W. H. Dickhoff, *Int. J. Mod. Phys. A* **24**, 2060 (2009).
- [66] A. Cipollone, C. Barbieri, and P. Navrátil, *Phys. Rev. C* **92**, 014306 (2015).
- [67] <https://github.com/GSMUTNSR>.